

# Search for the rare decay $K^+ \rightarrow \mu^+ \nu \bar{\nu} \nu$

A.V. Artamonov,<sup>1</sup> B. Bassalleck,<sup>2</sup> B. Bhuyan,<sup>3, a</sup> E.W. Blackmore,<sup>4</sup> D.A. Bryman,<sup>5</sup> S. Chen,<sup>6, 4</sup> I-H. Chiang,<sup>3</sup> I.-A. Christidi,<sup>7, b</sup> P.S. Cooper,<sup>8</sup> M.V. Diwan,<sup>3</sup> J.S. Frank,<sup>3, c</sup> T. Fujiwara,<sup>9</sup> J. Hu,<sup>4</sup> J. Ives,<sup>5</sup> A.O. Izmaylov,<sup>10</sup> D.E. Jaffe,<sup>3</sup> S. Kabe,<sup>11, d</sup> S.H. Kettell,<sup>3</sup> M.M. Khabibullin,<sup>10</sup> A.N. Khotjantsev,<sup>10</sup> P. Kitching,<sup>12</sup> M. Kobayashi,<sup>11</sup> T.K. Komatsubara,<sup>11</sup> A. Konaka,<sup>4</sup> Yu.G. Kudenko,<sup>10, 13, 14</sup> L.G. Landsberg,<sup>1, d</sup> B. Lewis,<sup>2</sup> K.K. Li,<sup>3</sup> L.S. Littenberg,<sup>3</sup> J.A. Macdonald,<sup>4, d</sup> J. Mildenerger,<sup>4</sup> O.V. Mineev,<sup>10</sup> M. Miyajima,<sup>15</sup> K. Mizouchi,<sup>9</sup> N. Muramatsu,<sup>16, e</sup> T. Nakano,<sup>16</sup> M. Nomachi,<sup>17</sup> T. Nomura,<sup>9, f</sup> T. Numao,<sup>4</sup> V.F. Obraztsov,<sup>1</sup> K. Omata,<sup>11</sup> D.I. Patalakha,<sup>1</sup> R. Poutissou,<sup>4</sup> G. Redlinger,<sup>3</sup> T. Sato,<sup>11</sup> T. Sekiguchi,<sup>11</sup> A.T. Shaikhiev,<sup>10</sup> T. Shinkawa,<sup>18</sup> R.C. Strand,<sup>3</sup> S. Sugimoto,<sup>11, d</sup> Y. Tamagawa,<sup>15</sup> R. Tschirhart,<sup>8</sup> T. Tsunemi,<sup>11, g</sup> D.V. Vavilov,<sup>1, h</sup> B. Viren,<sup>3</sup> Zhe Wang,<sup>6, 3</sup> Hanyu Wei,<sup>6</sup> N.V. Yershov,<sup>10</sup> Y. Yoshimura,<sup>11</sup> and T. Yoshioka<sup>11, i</sup>  
(E949 Collaboration)

<sup>1</sup>*Institute for High Energy Physics, Protvino, Moscow Region, 142 280, Russia*

<sup>2</sup>*Department of Physics and Astronomy, University of New Mexico, Albuquerque, NM 87131*

<sup>3</sup>*Brookhaven National Laboratory, Upton, NY 11973*

<sup>4</sup>*TRIUMF, 4004 Wesbrook Mall, Vancouver, British Columbia, Canada V6T 2A3*

<sup>5</sup>*Department of Physics and Astronomy, University of British Columbia, Vancouver, British Columbia, Canada V6T 1Z1*

<sup>6</sup>*Department of Engineering Physics, Tsinghua University, Beijing 100084, China*

<sup>7</sup>*Department of Physics and Astronomy, Stony Brook University, Stony Brook, NY 11794*

<sup>8</sup>*Fermi National Accelerator Laboratory, Batavia, IL 60510*

<sup>9</sup>*Department of Physics, Kyoto University, Sakyo-ku, Kyoto 606-8502, Japan*

<sup>10</sup>*Institute for Nuclear Research RAS, 60 October Revolution Prospect 7a, 117312 Moscow, Russia*

<sup>11</sup>*High Energy Accelerator Research Organization (KEK), Oho, Tsukuba, Ibaraki 305-0801, Japan*

<sup>12</sup>*Centre for Subatomic Research, University of Alberta, Edmonton, Canada T6G 2N5*

<sup>13</sup>*Moscow Institute of Physics and Technology, 141700 Moscow, Russia*

<sup>14</sup>*National Research Nuclear University MEPhI (Moscow Engineering Physics Institute), 115409 Moscow, Russia*

<sup>15</sup>*Department of Applied Physics, Fukui University, 3-9-1 Bunkyo, Fukui, Fukui 910-8507, Japan*

<sup>16</sup>*Research Center for Nuclear Physics, Osaka University,*

*10-1 Mihogaoka, Ibaraki, Osaka 567-0047, Japan*

<sup>17</sup>*Laboratory of Nuclear Studies, Osaka University,*

*1-1 Machikaneyama, Toyonaka, Osaka 560-0043, Japan*

<sup>18</sup>*Department of Applied Physics, National Defense Academy, Yokosuka, Kanagawa 239-8686, Japan*

(Dated: September 2, 2016)

Evidence of the  $K^+ \rightarrow \mu^+ \nu \bar{\nu} \nu$  decay was searched for using E949 (Brookhaven National Laboratory, USA) experimental data with an exposure of  $1.70 \times 10^{12}$  stopped kaons. The data sample is dominated by the background process  $K^+ \rightarrow \mu^+ \nu \mu \gamma$ . An upper limit on the decay rate  $\Gamma(K^+ \rightarrow \mu^+ \nu \bar{\nu} \nu) < 2.4 \times 10^{-6} \Gamma(K^+ \rightarrow \text{all})$  at 90% confidence level was set assuming the Standard Model muon spectrum. The data are presented in such a way as to allow calculation of rates for any assumed  $\mu^+$  spectrum.

PACS numbers: 14.60.St, 13.20.Eb

## I. INTRODUCTION

The  $K^+ \rightarrow \mu^+ \nu \bar{\nu} \nu$  decay involves four fermions and cannot occur in first order in the Standard Model (SM). Therefore, its investigation provides information about higher-order weak effects. The most recent calculation of this process in the framework of the SM has been done by D. Gorbunov and A. Mitrofanov [1]. The SM predicts an extremely low total rate for this process ( $\mathcal{O}(10^{-16})$ ).

The study of the  $K^+ \rightarrow \mu^+ \nu \bar{\nu} \nu$  decay can also provide information on two effects: a neutrino-neutrino interaction [2, 3] and a six-fermion interaction [4, 5]. The differential decay rates for  $K^+ \rightarrow \mu^+ \nu \bar{\nu} \nu$  are the following:

<sup>a</sup> Now at Department of Physics, Indian Institute of Technology Guwahati, Guwahati, Assam, 781 039, India.

<sup>b</sup> Now at Physics Department, Aristotle University of Thessaloniki, Thessaloniki 54124, Greece.

<sup>c</sup> Now at 1 Nathan Hale Drive, Setauket, New York 11733.

<sup>d</sup> Deceased.

<sup>e</sup> Now at Research Center for Electron Photon Science, Tohoku University, Taihaku-ku, Sendai, Miyagi 982-0826, Japan.

<sup>f</sup> Now at High Energy Accelerator Research Organization (KEK), Oho, Tsukuba, Ibaraki 305-0801, Japan.

<sup>g</sup> Now at Department of Physics, Kyoto University, Sakyo-ku, Kyoto 606-8502, Japan.

<sup>h</sup> Now at TRIUMF, 4004 Wesbrook Mall, Vancouver, British Columbia, Canada V6T 2A3.

<sup>i</sup> Now at Department of Physics, Kyushu University, Higashi-ku, Fukuoka 812-8581, Japan.

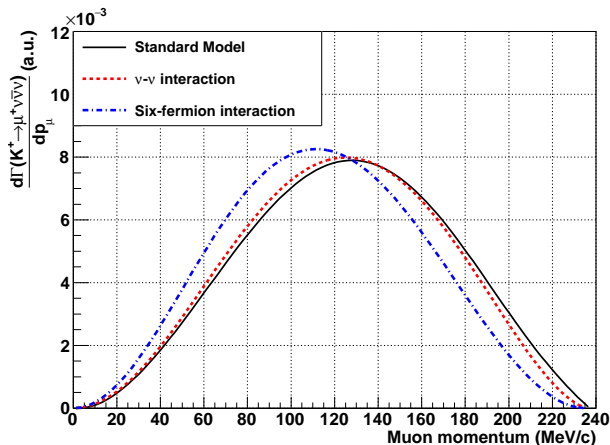


FIG. 1. Differential decay rates for  $K^+ \rightarrow \mu^+ \nu \bar{\nu} \nu$  process in the framework of the Standard Model,  $\nu$ - $\nu$  interaction model with  $F = 1$ , and six fermion interaction model with  $F_S = 1$ . All spectra are normalized to 1.

1. Neutrino-neutrino interaction.

$$\frac{d\Gamma}{dx} = \frac{1}{2^7 \pi^5} G^2 F^2 f_K^2 m_K (1 + r^2 - 2x)(x^2 - r^2)^{1/2} \times [(1 - 2x)x + r^2], \quad (1)$$

where  $r = m_\mu/m_K$ ,  $x = E_\mu/m_K$ ,  $E_\mu$  is the total muon energy,  $m_\mu$  and  $m_K$  are muon and kaon masses respectively,  $G$  is the Fermi constant,  $F$  is the hypothetical neutrino-neutrino interaction constant, and  $f_K$  is kaon decay constant.

2. Six fermion interaction.

$$\frac{d\Gamma}{dE_\mu} = f_K^2 F_S^2 2^9 R \left(1 + \frac{m_\mu}{E_\mu}\right),$$

$$R = \frac{m_K p_\mu A^2 E_\mu}{3\pi^5 2^{13}} (2p_\mu^3 + 4p_\mu^2 A + 2.5p_\mu A^2 + 0.5A^3),$$

$$A = m_K - E_\mu - p_\mu, \quad (2)$$

where  $f_K$  is kaon decay constant,  $E_\mu$  is the total muon energy,  $p_\mu$  is muon momentum,  $m_K$  is kaon mass,  $F_S$  is the common form factor which can be related to the usual four-fermion interaction constant  $G$  by the expression:

$$F_S = \frac{G}{\sqrt{2}} \frac{1}{\lambda^3}. \quad (3)$$

The constant  $\lambda$  is an unknown parameter with the dimension of mass.

According to [1] and Eq. (1, 2) the differential decay rates for  $K^+ \rightarrow \mu^+ \nu \bar{\nu} \nu$  decay are shown in Fig. 1. To compare the shape of the theoretical curves all spectra are normalized to 1.

The only direct search for the  $K^+ \rightarrow \mu^+ \nu \bar{\nu} \nu$  decay was done by C. Y. Pang *et al.* [6]. The muon kinetic energy

region  $60 < T_\mu < 100$  MeV was examined (corresponding to muon momentum region  $127.6 < p_\mu < 176.4$  MeV/c). No clear evidence of the signal decay was observed and a 90% C.L. upper limit was presented:

$$\frac{\Gamma(K^+ \rightarrow \mu^+ \nu \bar{\nu} \nu; 60 < T_\mu < 100 \text{ MeV})}{\Gamma(K^+ \rightarrow \text{all})} < 2.2 \times 10^{-6} \quad (4)$$

The 90% C.L. upper limits on total decay rate were obtained assuming the muon spectrum from neutrino-neutrino interaction and six-fermion interaction models:

1. Neutrino-neutrino interaction:

$$\frac{\Gamma(K^+ \rightarrow \mu^+ \nu \bar{\nu} \nu)}{\Gamma(K^+ \rightarrow \text{all})} < 6.0 \times 10^{-6}; \quad (5)$$

and

2. Six-fermion interaction:

$$\frac{\Gamma(K^+ \rightarrow \mu^+ \nu \bar{\nu} \nu)}{\Gamma(K^+ \rightarrow \text{all})} < 6.7 \times 10^{-6}. \quad (6)$$

The Eq. (5) is the best current upper limit on the  $K^+ \rightarrow \mu^+ \nu \bar{\nu} \nu$  decay rate.

In this paper, we present the result of a search for the rare kaon decay  $K^+ \rightarrow \mu^+ \nu \bar{\nu} \nu$  in the muon momentum region  $130 < p_\mu < 175$  MeV/c using stopped kaon decay data from experiment E949 at Brookhaven National Laboratory (BNL) [7]. In this analysis we used data taken from March to June in 2002. The total exposure for this analysis is  $1.70 \times 10^{12}$  stopped kaons [8]. This analysis is based on the search for heavy neutrinos,  $\nu_H$ , in the  $K^+ \rightarrow \mu^+ \nu_H$  decays [9] since in both cases a single muon must be identified. In the following the method of calculation of rates for any assumed  $\mu^+$  spectrum is also described.

## II. EXPERIMENT

The E949 experiment was aimed at a measurement of the rare kaon decay  $K^+ \rightarrow \pi^+ \nu \bar{\nu}$  [7] and other processes. Therefore, the principal trigger selection criteria were designed to select pions and reject muons. However, secondary muons were present in the data set due to inefficiencies in the pion selection criteria applied.

### A. Detector

The E949  $K^+$  beam was produced by a high-intensity proton beam from the Alternating Gradient Synchrotron at BNL. Protons were accelerated to a momentum of 21.5 GeV/c and hit a platinum production target.

The E949 detector is shown in Fig. 2. Incoming 710 MeV/c kaons with a  $K^+/\pi^+$  ratio of 3/1 were identified by a Čerenkov counter. Downstream of the Čerenkov

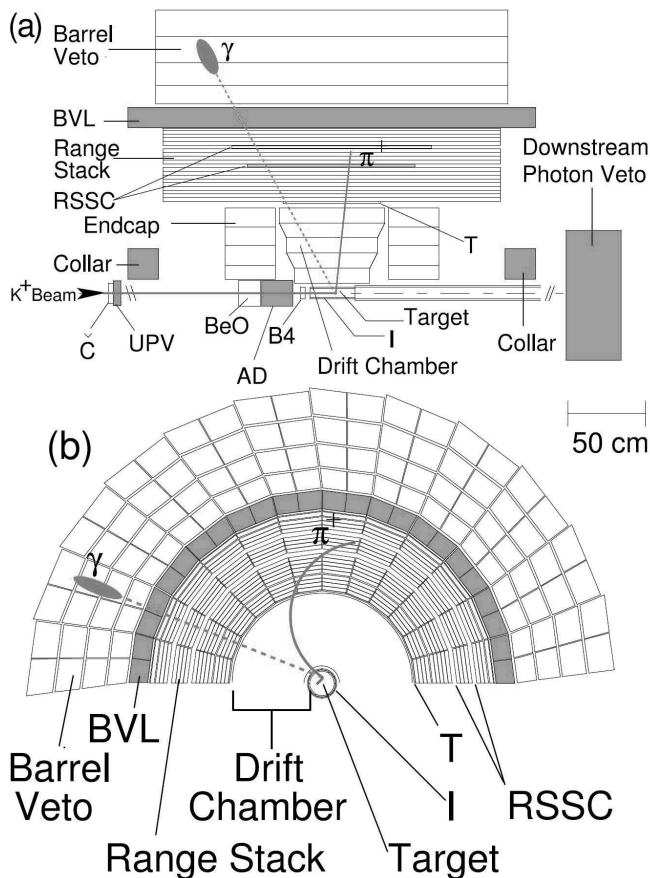


FIG. 2. Schematic side (a) and end (b) views of the upper half of the E949 detector. An incoming kaon is shown traversing the beam instrumentation, stopping in the target and decaying to  $\pi^+\pi^0$ . The outgoing charged pion and one photon from the  $\pi^0 \rightarrow \gamma\gamma$  decay are illustrated. Elements of the detector are described in the text.

counter was the upstream photon veto (UPV). The UPV was used to veto beam particles coincident with the time of the  $K^+$  decay. To monitor the beam profile and identify multiple incoming particle two proportional wire chambers (BWPCs) were used. Downstream of the BWPCs kaons were slowed down by a passive BeO degrader and an active degrader (AD). After passing through the degraders, a beam hodoscope (B4) detected the entrance position of beam particles into the target and identified it as a kaon by measuring the energy deposit. The slowed down kaons came to rest in the center of the target.

The target was a 12 cm diameter cylinder, 3.1 m in length, which was made of 413 5 mm square Bicon BCF10 scintillating fibers. These fibers ran in the direction parallel to the beam and had 0.09 mm thick inactive cladding. Smaller fibers, known as edge fibers, were used to fill the gaps near the outer edge of the target. Each of the 5 mm fibers was connected to a Hamamatsu R1635-02 photomultiplier tube (PMT). The edge fibers were multiplexed into groups of 12 and each group was read out by a single PMT. The PMT signals were sent to

analog-to-digital converters (ADCs), time-to-digital converters (TDCs) and charge-coupled devices (CCDs).

Typical energy deposits in an individual target fiber were on the order of tens of MeV for kaons traveling along the fiber, and only  $\sim 1$  MeV for pions (muons) passing perpendicularly through a fiber. The fiducial region of the target was defined by two layers of six plastic scintillator counters surrounding the target. The inner scintillators (IC) surrounded the target and tagged charged decay products before they entered the drift chamber. The IC was 6.4 mm thick with an inner radius of 6.0 cm and extended 24 cm from the upstream face of the target. The outer scintillators (VC) overlapped the downstream edge of the IC by 6 mm and detected particles that decayed downstream of the fiducial region of the target. The VC was 5 mm thick and 1.96 m long. To prevent gaps, the VC elements were rotated by  $30^\circ$  with respect to the IC elements. Each IC and VC element was read out by a PMT whose signal was sent to ADC, TDC and a 500 MHz transient digitizer (TD) based on a flash ADC.

The drift chamber, called the Ultra Thin Chamber (UTC), was located just outside of the IC, with an inner radius of 7.85 cm, an outer radius of 43.31 cm and length of 51 cm. The whole E949 spectrometer was in a 1 Tesla magnetic field. The primary functions of the UTC were the momentum measurement of charged particles and providing a match between the tracks in the target and the range stack explained in the next paragraph.

The Range Stack (RS) consisted of 19 layers of scintillator counters, azimuthally segmented into 24 sectors, and position-sensitive straw chambers embedded after the 10th and 14th layers of scintillator, and was located just outside of the UTC with an inner radius of 45.08 cm and an outer radius of 84.67 cm. The RS provided energy and range measurements. The innermost layer, T-counter, was 0.635 cm thick and 52 cm long. The T-counter defined the fiducial volume for the charged decay products and was thinner than the remaining RS layers to suppress the rate from photon conversions. Each of the T-counter scintillators was read out by fibers coupled to a PMT at both the upstream and downstream ends. Layers 2–18 were 1.905 cm thick and 1.82 m long and each scintillator was coupled through light guides to PMTs at each end. Layer 19 was used mainly to veto long range charged particles such as muons. This layer was 1.0 cm thick and had the same length and read out method as layers 2–18.

The detection of any activity coincident with the charged track was important for suppressing the backgrounds for  $K^+ \rightarrow \mu^+\nu\bar{\nu}\nu$  decay. The E949 detector included a hermetic system of photon veto detectors. Nearly every detector subsystem contributed to the photon veto. Detectors whose sole purpose was the detection of photon activity were the Barrel Veto (BV), the Barrel Veto Liner (BVL), the upstream and downstream End Caps, the upstream and downstream Collars, the down-

stream Microcollar ( $\mu\text{CO}$ ) and the Downstream Photon Veto. Detectors that were part of the photon veto system, but also served other purposes were the AD, target, IC, VC and RS. For a given event, the regions of the target, IC and RS traversed by the charged track were excluded from the photon veto. The BV and BVL with thicknesses of 14.3 and 2.29 radiation lengths (r.l.) at normal incidence, respectively, provided photon detection over  $2/3$  of the  $4\pi$  solid angle. The photon detection over the remaining  $1/3$  of the  $4\pi$  solid angle was provided by the other calorimeters in the region from  $10^\circ$  to  $45^\circ$  of the beam axis with a total thickness from 7 to 15 r.l.

### B. The $K^+ \rightarrow \mu^+ \nu \bar{\nu}$ trigger

The experimental signature of the  $K^+ \rightarrow \mu^+ \nu \bar{\nu}$  decay is similar to the  $K^+ \rightarrow \mu^+ \nu_H$  decay (one single charged track with no other detector activity). This motivates the use of the same trigger. To search for a heavy neutrino we used the main E949 trigger [9]. This trigger consisted of several requirements. First, a kaon had to enter the target. To be sure that the kaon decayed at rest, the secondary charged particle had to leave the target at least 1.5 ns later than the kaon hit in the Čerenkov detector. The 3-body  $K^+$  decays were suppressed by the RS layer requirements. The charged particle had to reach at least the sixth layer of the RS (Fid&Range). Long tracks (e.g. from  $K^+ \rightarrow \mu^+ \nu_\mu$  decays) were suppressed by the layer 19 veto requirement. There were also additional refined requirements of the charged track range took into account the number of target fiber hits and the track's downstream position in RS layers 3, 11, 12, 13 as well as the deepest layer of penetration (refined range). The charged track had to be within the fiducial region of all traversed RS layers.

The main trigger included the online pion identification in the RS. It required a signature of  $\pi^+ \rightarrow \mu^+ \nu_\mu$  decay in the online-selected stopping counter. The  $\mu^+$  from the  $\pi^+ \rightarrow \mu^+ \nu_\mu$  decay-at-rest had the kinetic energy of 4 MeV (few mm equivalent range in plastic scintillator) and rarely exited the stopping counter. So, pion pulses in the stopping counter recorded by transient digitizers had a double-pulse structure. Despite the online pion identification requirement, some muons remained in the final sample due to inefficiency.

Events were rejected if any activity in the photon detectors with energy above a threshold was detected. This condition removed events with photons. A similar requirement in the RS was also applied. The 24 sectors of the RS were grouped into six; a group of 4 sectors was called a "hextant". Only one hextant was allowed to have hits or two hextants if they were adjacent. This rejected events with multiple tracks and events with photon activity in the RS.

A more detail description of the E949 experiment can be found in [7, 10].

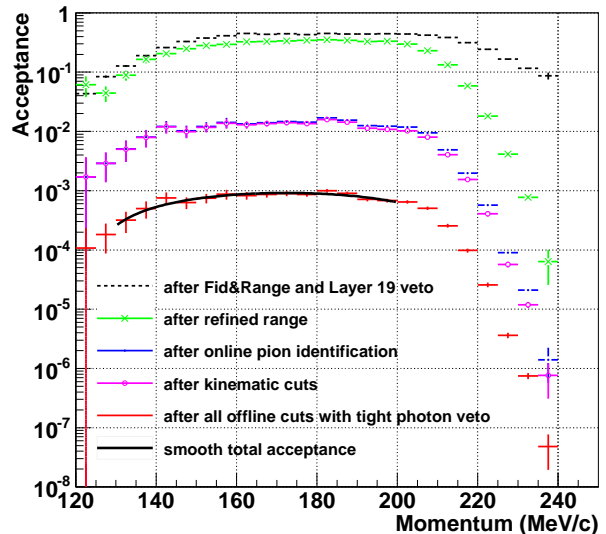


FIG. 3. Acceptance dependence on muon momentum. Black solid line shows the smooth total acceptance which is used for the further analysis.

## III. ANALYSIS

### A. Event selection

In addition to the online selection criteria, offline selection criteria were also applied to suppress background processes and select single muon tracks. These criteria were exactly the same as for the heavy neutrinos search [9] since the experimental signature of the  $K^+ \rightarrow \mu^+ \nu \bar{\nu}$  decay is similar to the  $K^+ \rightarrow \mu^+ \nu_H$  decay. The acceptances of all selection criteria were measured using muon samples from the  $K^+ \rightarrow \mu^+ \nu_\mu$  and  $K^+ \rightarrow \mu^+ \nu_\mu \gamma$  decays passed through monitor triggers. The description of acceptance measurements may be found in [9]. The total acceptance after all cuts is shown in Fig. 3. The acceptance drop off below 140 MeV/c is due to the requirement that the charged track must reach at least the sixth layer of the RS. The acceptance drop off above 200 MeV/c is due to two requirements. First, the charged track must not reach layer 19 of the range stack and second, the refined range removes long tracks which are dominant at high momentum for events passing the layer 19 requirement. The main acceptance loss (factor  $\sim 20$ ) comes from the online pion identification requirement (see Figure 3).

### B. The $K^+ \rightarrow \mu^+ + X$ branching ratio

The muon momentum spectrum for the full E949 data sample after all selection criteria is shown in Fig. 4. The data sample is dominated by the peak events at  $p_\mu = 236$  MeV/c (muons from the  $K^+ \rightarrow \mu^+ \nu_\mu$  decay) and

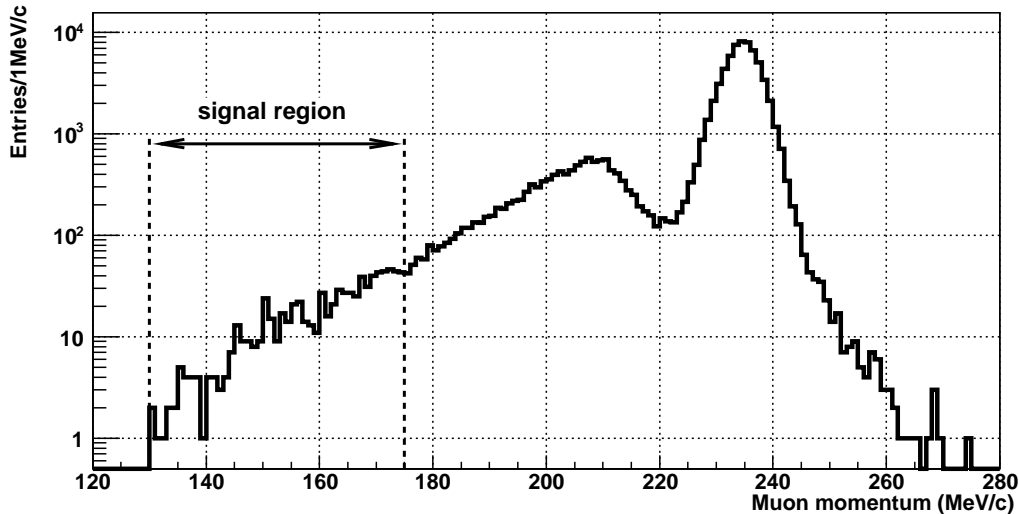


FIG. 4. Muon momentum spectrum for the full E949 data sample after all selection criteria were applied. The signal region is from 130 to 175 MeV/c.

muons from the  $K^+ \rightarrow \mu^+ \nu_\mu \gamma$  decay [9]. Therefore, the main background source for the process  $K^+ \rightarrow \mu^+ + X$ , where  $X$  is set of neutral undetectable particles, is  $K^+ \rightarrow \mu^+ \nu_\mu \gamma$  decay. Since we are not able to accurately predict the number of the background events after all selection criteria, we calculated the standard one-sided 90% C.L. upper limits (assuming gaussian distribution of measured values) on the signal process for different signal regions based on the observed events:

$$BR_P(K^+ \rightarrow \mu^+ + X) < \frac{1}{N_K} \sum_{i=130}^P \frac{N_i}{Acc_i} + 1.28\sigma, \quad (7)$$

where  $N_i$  is the number of observed events in the  $i$ th bin (Fig. 4),  $Acc_i$  is the total acceptance for the  $i$ th bin (Fig. 3),  $N_K$  is the number of stopped kaons,  $\sigma$  is the total error which takes into account both uncertainties on  $Acc_i$ ,  $N_i$  and correlation between selected bins. The acceptance systematic uncertainty equals  $\simeq 30\%$  of the acceptance value [9]. The lowest bound of the signal region, 130 MeV/c, was selected due to the acceptance drop off (Fig. 3). The upper bound of the signal region,  $P$ , was varied up to 200 MeV/c (limited by acceptance measurements). To get total decay rate from Eq. (7) we need to know the expected muon momentum spectrum. For any assumed spectrum the total decay rate on  $K^+ \rightarrow \mu^+ \nu \bar{\nu}$  decay can be calculated using the following expression:

$$\frac{\Gamma(K^+ \rightarrow \mu^+ \nu \bar{\nu})}{\Gamma(K^+ \rightarrow \text{all})} = BR_P(K^+ \rightarrow \mu^+ + X) \times \frac{\int_0^{p_\mu^{max}} (d\Gamma/dp_\mu) dp_\mu}{\int_{130}^P (d\Gamma/dp_\mu) dp_\mu}, \quad (8)$$

where  $BR_P(K^+ \rightarrow \mu^+ + X)$  is defined by Eq. (7),  $p_\mu^{max}$  is the maximum muon momentum defined by kinematics ( $p_\mu^{max} = (m_K^2 - m_\mu^2)/2m_K$ ). Using the SM spectrum [1] and Eq. (1, 2, 8), the total acceptance distribution from Fig. 3 and  $N_K = 1.70 \times 10^{12}$  we derived upper limits on the  $K^+ \rightarrow \mu^+ \nu \bar{\nu}$  branching ratio for different signal regions (Fig. 5).

#### IV. RESULTS

The number of observed events is drastically increased with muon momentum as shown in Fig. 4. So, the upper bound of the signal region, 175 MeV/c, was selected to correspond to the previous experimental search for the  $K^+ \rightarrow \mu^+ \nu \bar{\nu}$  decay [6].

Using Eq. (7) with  $P = 175$  MeV/c we get the following upper limit on the partial  $K^+ \rightarrow \mu^+ + X$  branching ratio:

$$BR(K^+ \rightarrow \mu^+ + X, 130 < p_\mu < 175 \text{ MeV/c}) < 7.5 \times 10^{-7} \quad (9)$$

To get total decay rate from Eq. (9) we used Eq. (8):

$$\frac{\Gamma(K^+ \rightarrow \mu^+ \nu \bar{\nu})}{\Gamma(K^+ \rightarrow \text{all})} = 7.5 \times 10^{-7} \times \frac{\int_0^{p_\mu^{max}} (d\Gamma/dp_\mu) dp_\mu}{\int_{130}^{175} (d\Gamma/dp_\mu) dp_\mu}, \quad (10)$$

Using the SM spectrum [1] and Eq. (1, 2, 10) we get the following 90% C.L. upper limits on the total decay rate for  $K^+ \rightarrow \mu^+ \nu \bar{\nu}$  decay:

##### 1. Standard Model.

$$\frac{\Gamma(K^+ \rightarrow \mu^+ \nu \bar{\nu})}{\Gamma(K^+ \rightarrow \text{all})} < 2.4 \times 10^{-6} \quad (11)$$

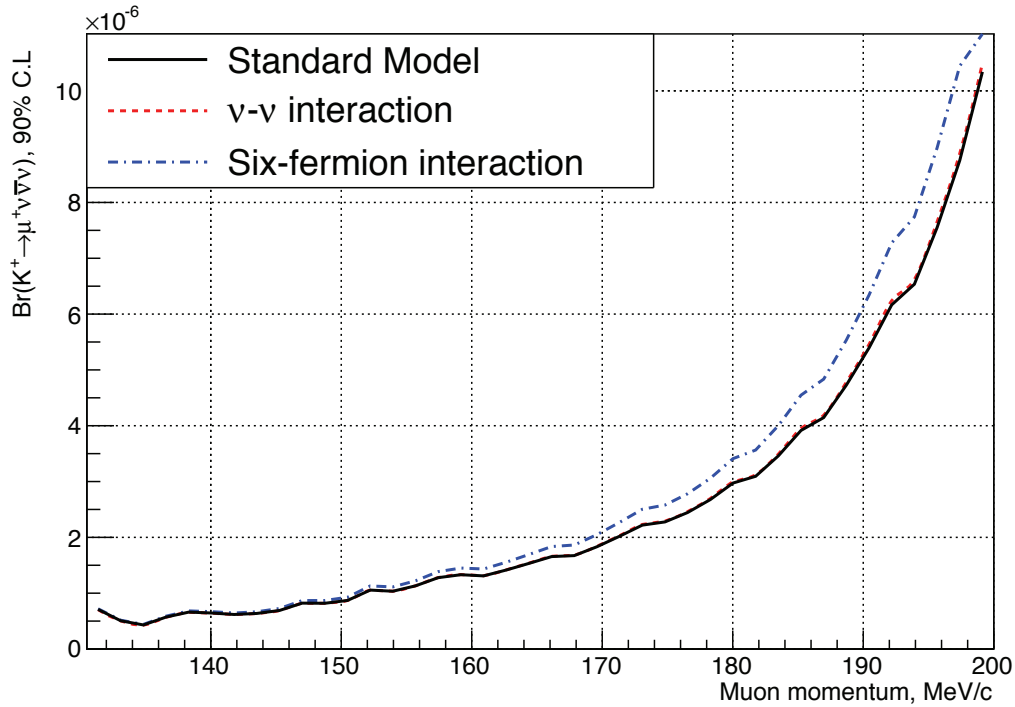


FIG. 5. Upper limits on the  $K^+ \rightarrow \mu^+ \nu \bar{\nu} \nu$  branching ratio for the signal region 130- P MeV/c, where P is x-axis value.

2. Neutrino-neutrino interaction.

$$\frac{\Gamma(K^+ \rightarrow \mu^+ \nu \bar{\nu} \nu)}{\Gamma(K^+ \rightarrow \text{all})} < 2.4 \times 10^{-6} \quad (12)$$

3. Six-fermion interaction:

$$\frac{\Gamma(K^+ \rightarrow \mu^+ \nu \bar{\nu} \nu)}{\Gamma(K^+ \rightarrow \text{all})} < 2.7 \times 10^{-6} \quad (13)$$

As can be seen from comparison of Eq. (11, 12, 13) with Eq. (5, 6) the results obtained with E949 data allow improvement of the limits on the  $K^+ \rightarrow \mu^+ \nu \bar{\nu} \nu$  decay by about a factor of 3.

## V. CONCLUSION

A search for the rare decay  $K^+ \rightarrow \mu^+ \nu \bar{\nu} \nu$  was done in the muon momentum region  $130 < p_\mu < 175$  MeV/c using E949 data. No evidence of this process was found and

we set new 90% C.L. upper limit on the decay rate. Two proposed muon momentum spectra, neutrino-neutrino interaction and six-fermion interaction, were considered and we improved the current limits on the total decay rate in the framework of these models and for the Standard Model. We also presented the method of calculation of total rates on the  $K^+ \rightarrow \mu^+ \nu \bar{\nu} \nu$  process for any assumed muon momentum spectrum.

## ACKNOWLEDGMENTS

This research was supported in part by Grant #14-12-00560 of the Russian Science Foundation, the U.S. Department of Energy, the Ministry of Education, Culture, Sports, Science and Technology of Japan through the Japan-U.S. Cooperative Research Program in High Energy Physics and under Grant-in-Aids for Scientific Research, the Natural Sciences and Engineering Research Council (Grant no. 157985) and the National Research Council of Canada, National Natural Science Foundation of China, and the Tsinghua University Initiative Scientific Research Program.

[1] D. Gorbunov and A. Mitrofanov, “ $K^+ \rightarrow \mu^+ \nu_\mu \bar{\nu} \nu$  and  $K^+ \rightarrow e^+ \nu_e \bar{\nu} \nu$  decays within the chiral perturbation theory,” e-print: arXiv:1605.08077 [hep-ph].

[2] D.Yu. Bardin, S.M. Bilenky, and B. Pontecorvo, “On the  $\nu - \nu$  interaction,” Phys. Lett. **B32**, 121–124 (1970).

[3] M.S. Bilenky and A. Santamaria, “‘Secret’ neutrino interactions,” in *Neutrino mixing. Festschrift in honour*

- of Samoil Bilenky's 70th birthday. *Proceedings, International Meeting, Turin, Italy, March 25-27, 1999* (1999).
- [4] T.E.O. Ericson and S.L. Glashow, "Six-fermion weak interactions," *Phys. Rev.* **133**, B130–B131 (1964).
- [5] A. Vanzha, A. Isaev, and L. Lapidus, "On possible properties of weak six-fermion interaction," *Sov. J. Nucl. Phys.* **12**, 325 (1971).
- [6] C.Y. Pang, R.H. Hildebrand, G.D. Cable, and R. Stiening, "Search for rare  $K^+$  decays. I.  $K^+ \rightarrow \mu^+ \nu \bar{\nu}$ ," *Phys. Rev.* **D8**, 1989–2003 (1973).
- [7] A.V. Artamonov *et al.* (E949 Collaboration), "Study of the decay  $K^+ \rightarrow \pi^+ \nu \bar{\nu}$  in the momentum region  $140 < P_\pi < 199$  MeV/c," *Phys. Rev.* **D79**, 092004 (2009).
- [8] This is slightly less than  $1.71 \times 10^{12}$  stopped kaons used for the E949 analysis [7].
- [9] A.V. Artamonov *et al.* (E949 Collaboration), "Search for heavy neutrinos in  $K^+ \rightarrow \mu^+ \nu_H$  decays," *Phys. Rev.* **D91**, 052001 (2015).
- [10] S. Adler *et al.*, "Measurement of the  $K^+ \rightarrow \pi^+ \nu \nu$  branching ratio," *Phys. Rev.* **D77**, 052003 (2008).